

Multiple crack detection of pipes using PZT-based guided waves

*Shi Yan¹⁾, Ji Qi²⁾, Nai-Zhi Zhao³⁾, Yang Cheng⁴⁾ and Sheng-Wenjun Qi⁵⁾

^{1), 2), 3), 4)} *School of Civil Engineering, Shenyang Jianzhu University, Shenyang Liaoning
110168, China*

⁵⁾ *School of Civil and Environmental Engineering, Beijing University of Technology,
Beijing 100081, China*

¹⁾ *syang1962@163.com*, ²⁾ *870097320@qq.com*, ³⁾ *zhaonaizhi@163.com*

ABSTRACT

This paper focuses on the multiple crack detection of steel pipelines using PZT-based guided waves. Numerical simulations of cracked pipes based on ultrasonic guided-waves are conducted by using the ANSYS finite element software. The pipe model has been established and multiple cracks have been artificially simulated. The excitation signal is applied as a movement of displacement at one end of the pipe along the pipe length direction to simulate the guided waves of L mode which could be generated by a ring of surface-pasted PZT actuators. Based on the analysis of the reflected signal, the arrival time of the crack reflection waves are determined and the crack positions are accurately evaluated by the calculation of the travel time and group velocity of the PZT-based guided waves. The crack parameters are numerically altered to determine how the parameters impact the sensitive degree of the pipe crack damage. To validate the efficiency of the numerical simulation, an experiment of the multiple crack detection for the same parameter pipe with the numerical model is performed in the laboratory, and the results match well with the numerical simulation.

1. INTRODUCTION

Pipeline has become one of the five forms of transport to keep pace with the railway, highway, aviation, water transportation (Zang 1998), which possesses many advantages, such as low cost delivery, large capacity, short construction period, small area of land occupation, safety, no pollution, and works in a harsh natural environmental condition and automatic way of transportation. However, most of pipes might be working in a harsh environment, and subjected to a corrosion condition in the long-term use,

which is extremely susceptible to generate degradation, corrosion and perforation, cracks and other defects. The typical defects of pipeline structures are shown in Fig.1. These defects may result in lowering the security of the pipeline working, and eventually lead to leakage, even explosion accidents. Therefore, it is of importance to develop the defect detection method for pipeline structures by using an effective way such as the PZT-based guided waves.

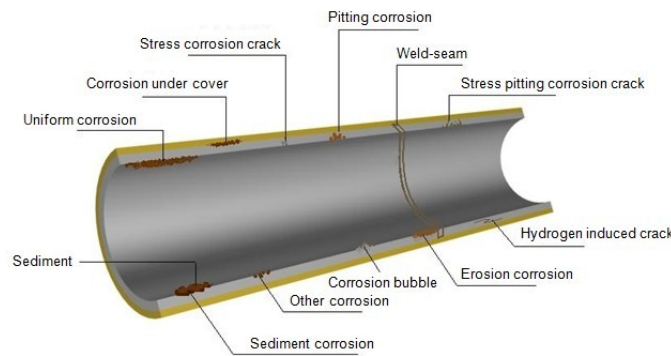


Fig. 1 The schematic of typical defects of pipeline structure

Many researchers have studied defect detection methods by using guided waves. Gazis (Gazis 1959) solved an issue of a harmonic wave propagating in an infinite length hollow cylinder by the elastic theory, successfully explained the frequency dispersion and multi-mode phenomena of the guided wave, which is a start sign of the guided wave propagation research. Greenspon (Greenspon 1960) systematically developed the dispersion curves and displacement field for a cylindrical shell. Silk (Silk 1979) successfully divided the guided wave in a cylindrical shell into axially symmetric longitudinal modes of $L(0, m)$, axially symmetric torsional modes of $T(0, m)$ and asymmetric bending modes of $F(n, m)$, and this classification has been in use now. The guided wave technology has made a considerable development from 1980s. The guided wave technology based on corrosion damage detections of pipeline structures has rapidly developed and focused on the damage identification of laminated composite structures. Lowe (Lowe 1998) derived dispersion equations for guided wave propagating in laminated hollow cylinder. In China, the research has been successful in the field. Du (Du 2004) derived the generalized frequency equation for axisymmetric guided waves in a two layered cylindrical composite structure with a weak interface by using the spring model for a weak interface. Liu (Liu 2006, 2007) theoretically and experimentally researched the inviscid liquid-filled pipe by using PZT-based guided

waves, and the results show that the water-infilled steel pipe has the properties of mode branching and group velocity decreasing.

However, pipeline damages such as cracks are not a single one; therefore, there is a need to further study the position and damage level of multiple cracks.

2. BASIC THEORY

2.1 Piezoelectric Effects and Equations

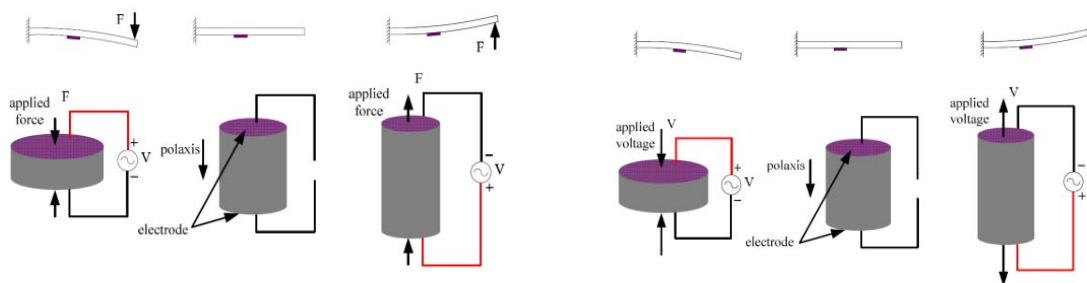
Piezoelectric ceramics material has the positive and converse piezoelectric effects, which can be used as both the signal transmission actuator and the signal reception sensor, shown in Fig.1 (a) and (b). Therefore, the piezoelectric equation is expressed for the positive piezoelectric effect, as shown in Eq. (1)

$$\{T\} = [c^E] \{S\} - [e^t] \{E\} \quad (1)$$

For the converse piezoelectric effect, the piezoelectric equation is shown in Eq. (2).

$$\{D\} = [e] \{S\} - [\epsilon^S] \{E\} \quad (2)$$

Where, $[c^E]$ is the elastic stiffness constant matrix; $[\epsilon^S]$ is the clamping dielectric constant matrix; $[e]$ is the piezoelectric stress constant matrix, $[e^t]$ is the transposed matrix of e ; $\{T\}$ is the stress vector; $\{S\}$ is the strain vector; $\{E\}$ is the electric field strength vector; $\{D\}$ is the electric displacement vector.



(a) Positive piezoelectric effect-sensor (b) Converse piezoelectric effect-actuator

Fig.2. The schematic of piezoelectric effects

The PZT4 piezoelectric ceramics is selected in this paper to make the PZT-based transducer. Each wafer is 12mm long, 6mm wide and 1mm thick.

2.2 PZT-based Guided Waves

When ultrasonic is limited within the boundaries of ruled materials such as plates, rods and pipes, it goes through multiple reflections on the border and interferences through the media. That forms the guided waves. Group velocity and phase velocity are not only the two basic concepts of the guided wave theory but also the main parameters of guided waves. Ultrasonic guided waves always spread with the group velocity and the group velocity is the speed of wave group energy. According to the knowledge of elasticity and the condition of freedom, the wave equation is shown in Eq. (3) and (4), respectively.

$$\frac{\partial \sigma_r}{\partial r} + \frac{\sigma_r - \sigma_\theta}{r} + \frac{1}{r} \cdot \frac{\partial \sigma_{r\theta}}{\partial \theta} + \rho \cdot \omega^2 \cdot u_r = 0 \quad (3)$$

$$\frac{\partial \sigma_{r\theta}}{\partial r} + \frac{1}{r} \cdot \frac{\partial \sigma_\theta}{\partial \theta} + 2 \cdot \frac{\sigma_{r\theta}}{r} + \rho \cdot \omega^2 \cdot u_\theta = 0 \quad (4)$$

In which, r and θ are the radial component of the cylindrical coordinate system, ω is circular frequency of the wave, ρ is the density of material, u is the displacement component, σ is the stress component.

2.3 Dispersion Curves of Guided Waves

Guided waves usually have two basic characteristics: dispersion and multi-modal characteristics. Guided waves in a pipe can be divided into longitudinal mode (L mode), torsional mode (T mode) and flexural mode (F mode). Based on linear elastic theory, Gazis (Gazis 1959) put forward the dispersion equation of harmonics transmitting in the infinitely long hollow pipe, shown in Eq. (5).

$$|C_{ij}|_{6 \times 6} = 0 \quad (5)$$

Where, C_{ij} is the coefficient which is associated with the wave number k and circular frequency ω . Gazis (Gazis 1959) gave the analytical expression and indicated that the Eq. (5) is a kind of transcendental equation and can be solved by numerical method. By using the numerical method to solve this determinant equation, the relationship among frequency, phase velocity and group velocity, expressed by the dispersion curve, can be obtained (Hong 2009). Based on the steel pipe with the diameter of 70mm, wall thickness of 4 mm, the dispersion curve is shown in Fig. 3.

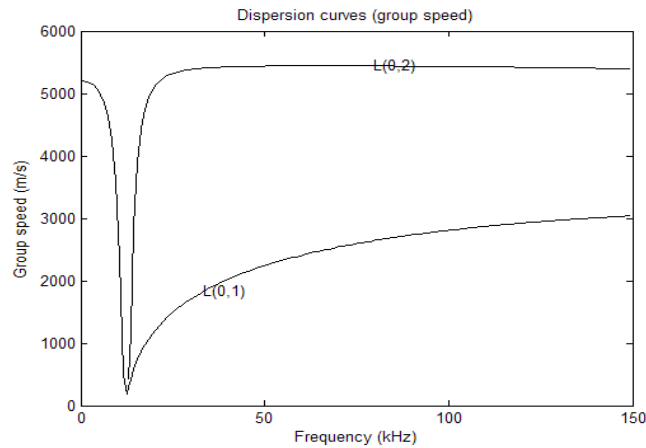


Fig. 3 Dispersion curve of L mode for a hollow steel pipe

We can see that guided waves travel along with the change of frequency. The number of guided wave mode is not less than two at any frequency and increases rapidly with the increase of the frequency.

2.4 Physical Model

An internal hollow steel pipe is selected in this paper as a research object to carry on the numerical simulation and experimental study, aiming at finding an effective way to indentify multi-cracks in the pipe. For the use of numerical simulation and experimental validation, a physical model is set up and the material parameters are shown in Table 1.

Table 1 Material parameters of steel pipe

| Modulus of elasticity E | Poisson ratio μ | Density ρ |
|---------------------------|---------------------|-----------------------|
| 210GPa | 0.32 | 7850kg/m ³ |

Based on PZT-based guided waves, the numerical simulation for multiple cracks detection of the pipeline in this paper is divided into three categories:

Category I: Two cracks paralleling to the circumferential direction are artificially set up in the pipe to identify the accurate location of defects.

Category II: The shell elements are selected to simulate the damage of the pipe. By altering the crack length and width, the law how the length and width of cracks impact on the sensitivity degree of pipe cracks is found out.

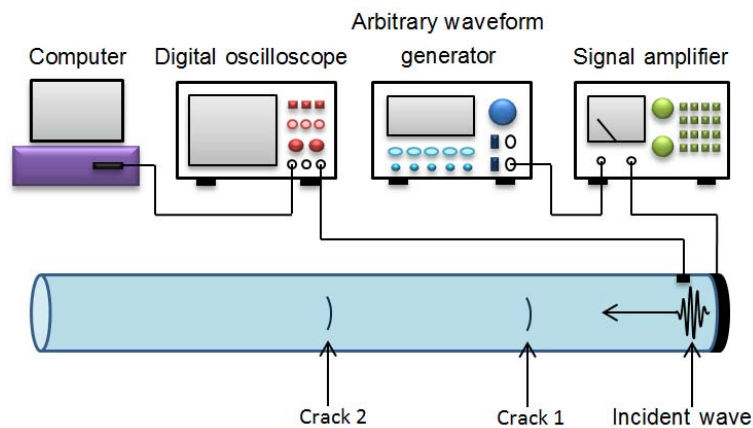
Category III: The solid elements are selected to simulate undermine pipes. With the alteration of the crack thickness, the law how thickness of cracks impacts the sensitive degree of pipe crack damage is found out.

3. EXPERIMENTAL STUDY

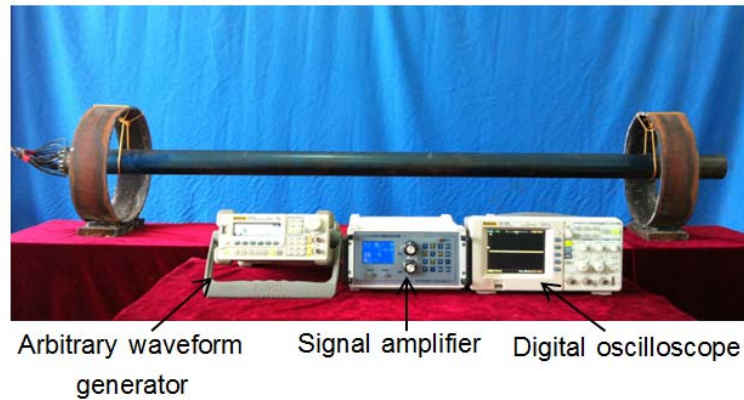
3.1 Experimental Setup

Pipeline structures in which the work environment is usually quite poor are greatly influenced by environmental erosion. Combined with the effect of artificial factor, it will produce various kinds of defects. Considering the damage form of multiple cracks which may exist in pipeline, the experiment of a double crack damage pipe is carried out in this paper, to determine the respective position of two cracks in the pipeline and establish a basis for the numerical simulation below.

During the experiment, arbitrary waveform generator, signal amplifier, digital oscilloscope and other equipment are used to establish an experimental system. The experimental setup is shown in Fig.4.



(a) The schematics of the experiment



(b) Experimental setup

Fig. 4 The schematics and the experimental setup

In order to suppress the influence of the flexural mode in the longitudinal mode (L mode), 16 pieces of PZT patches are arranged and pasted with the equal space on the surface at the end of the pipe along the circumferential direction. The sensor placement is shown in Fig. 5.

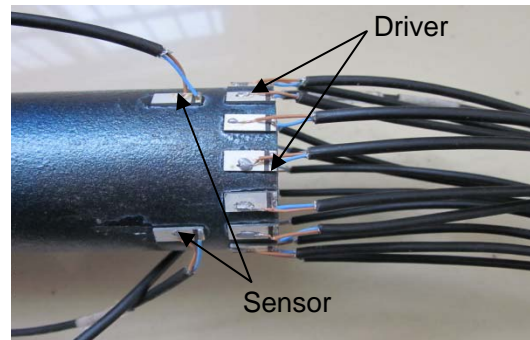
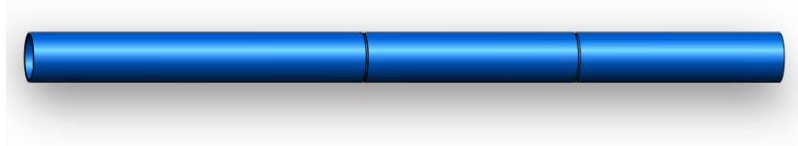


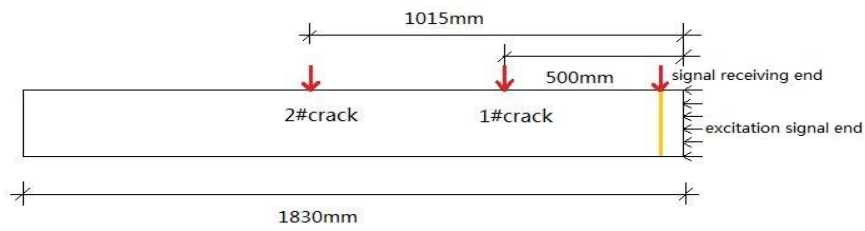
Fig. 5 PZT-based sensor placement

3.2 Experimental Process and Main Results

The dimension of the experimental pipe and the location of the artificial cracks are shown in Fig. 6.



(a) The experimentally used steel pipe



(b) Position of cracks

Fig.6 Steel pipe and two artificial cracks position

According to the dispersion characteristics of the PZT-based guided wave in the experimental pipeline, the sinusoidal signal of 70 kHz modulated by the Hanning window is selected as the excitation signal, shown in the Eq. (6).

$$x(t) = [1 - \cos(\frac{2 \cdot \pi \cdot f_c \cdot t}{n})] \cdot \sin(2 \cdot \pi \cdot f_c \cdot t) \quad (6)$$

Where, n is the number of the single signal, f_c is center frequency of the signal. The signal received in the receiving position is shown in Fig. 7.

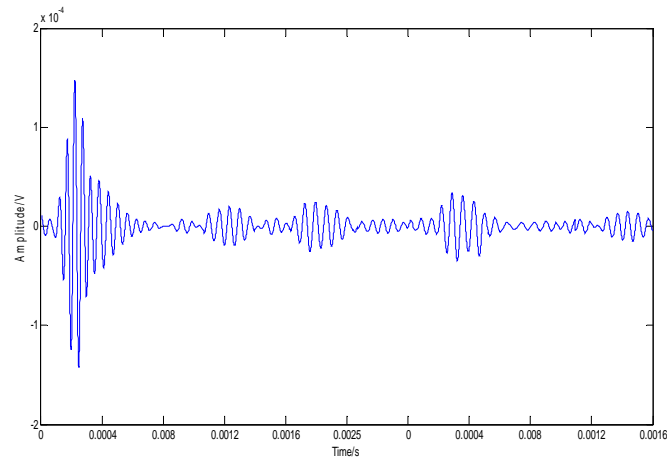


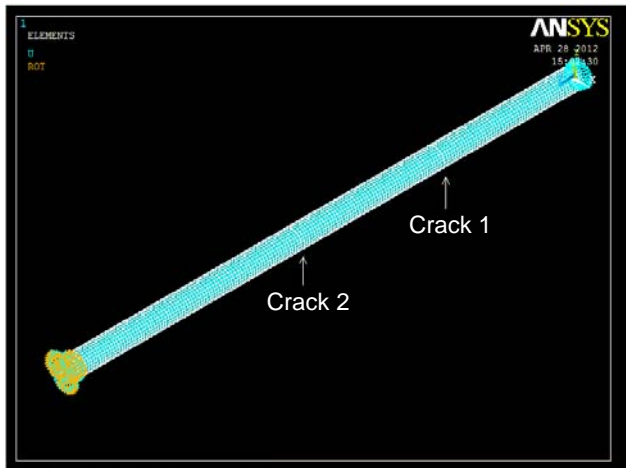
Fig. 7 Displacement-time curves of superimposed signal

According to the Young's speed of the guided wave propagated in the pipeline, $c_g=5440\text{m/s}$, it is calculated that the distances between the cracks and the receiving point for the Crack 1 and the Crack 2 are 0.5096m and 2 is 1.0366m, respectively. Compared with the actual measurement for the experimental pipe, the relative error is 1.92% and 2.13%, respectively. The cause of the error is considered from two ways. One is from the difference between the Young's speed calculated and the actual propagation velocity of the guided wave in the pipe. The other is that the time between defect echo and incident wave is different from the actual time.

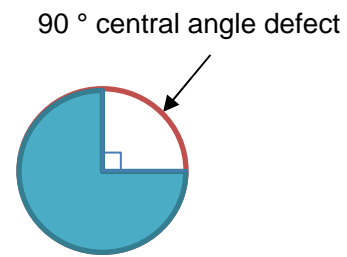
4. NUMERICAL SIMULATION

4.1 Simulation of Two Cracks Detection

The solid model for the finite element analysis (FEA) is established according to the above-mentioned experiment. All material parameters and boundary condition are the same to the experimental pipe. For the FEA, the shell-63 unit is selected. The pipe model section radius is 35mm and the wall thickness is 4mm. To simulate the defect, the degree of central angle is used to measure the size of defect, and two cracks are simulated in the same way, shown in Fig. 8.



(a) Finite element pipe model



(b) The degree of central angle

Fig. 8 The model meshing and the degree of central angle

To simulate the guided waves actuated by PZT transducers at the end of the pipe, axial instantaneous dynamic displacement load, which can be described by Eq. (6), is applied on each node at the end of the pipe as the initial excitation signal. The Full method is chosen to analyze the transient dynamics problem. The total propagating time is 1.2 ms , and the load action time is $100\ \mu\text{s}$, and the time step length is $1.2\ \mu\text{s}$.

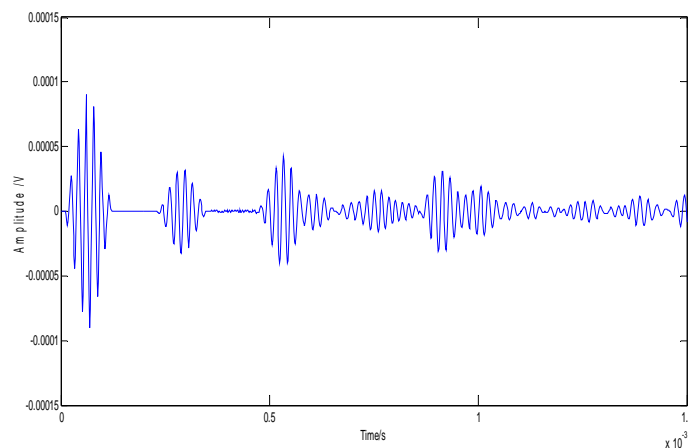


Fig. 9 Displacement-time curves of superimposed signal

Because of two cracks in pipeline, the conversion mode will make flaw echo difficult to identify. In order to eliminate the influence of defect echo (Lowe 1998), we can

average the receiving signal of each node which is located in the circumference of the pipeline. The averaged signal is shown in Fig.9.

The crack location and relative error is shown in Table 2.

Table 2 Crack location

| | 1#crack | 2#crack |
|---|-----------|------------|
| Calculation position from the receiving end | 0.503869m | 1.0029598m |
| Actual position from the receiving end | 0.5m | 1.015m |
| Relative error | 0.7738% | 1.186% |

According to the comparison of the displacement-time curves of the simulated signal and the experimental one, we can see that the numerical simulation method is feasible and accurate. From the relative error of Table 2, the calculated defect position and its actual position are basically consistent.

4.2 Impact of Cracks Length

According to the above-mentioned modeling method, pipes with cracks of 45, 60, 80 and 90 degree of central angles are simulated, respectively. In order to identify the sensitivity for the pipe to the defect length, width and depth, the concept of transmission coefficient is introduced, and its expression is shown in Eq. (7).

$$R = \frac{V_0 - V}{V_0} \quad (7)$$

In which, R is the transmission coefficient, V_0 is the incident wave amplitude value, V is the flaw echo amplitude value.

In order to intuitively compare relations between the crack length and transmission coefficient, transmission coefficients for cracks of different degree of central angles are calculated and the curve is plotted, shown in Fig. 10. From Fig. 10, we can clearly see that, with increase of the defect degree of central angle, the flaw echo amplitude value increases gradually, the end echo and the defect reflection coefficient gradually decrease, respectively, and the end transmission coefficient increases gradually under the condition of the same amplitude value of incident waves.

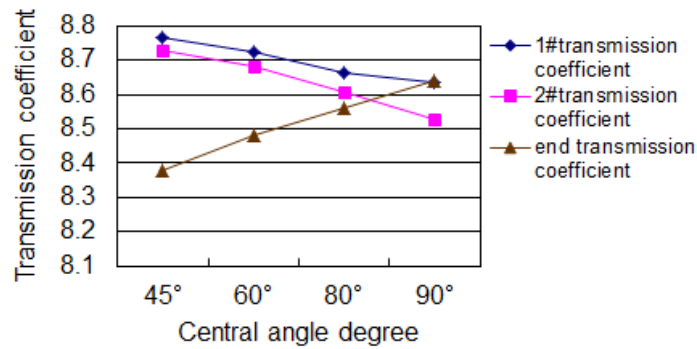


Fig. 10 Different transmission coefficient of different length cracks

4.3 Impact of Crack Width

According to the above-mentioned modeling method, pipes with 1.5mm, 2.0mm, 2.5mm and 3.0mm cracks are numerically simulated, respectively. Different flaw echo amplitude values and transmission coefficients are calculated with different defect width by using the same analysis method.

The relationship between crack widths and transmission coefficients is shown in Fig. 11.

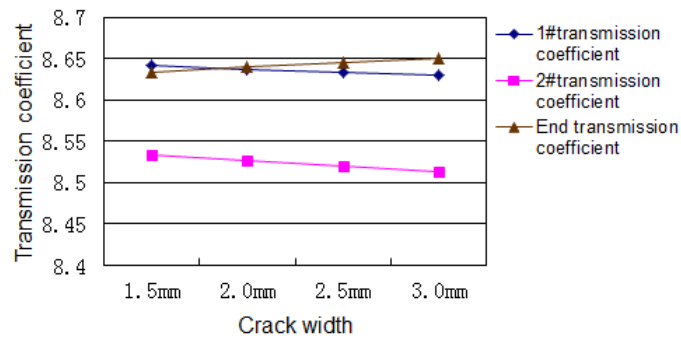


Fig. 11 Transmission coefficients vs. different width cracks

We can obviously see that with the increase of crack widths, incident wave amplitude values and flaw echo amplitude value increase, respectively, and the end echo amplitude decreases gradually, but the change is very small. The defect transmission coefficients decrease gradually, the end transmission coefficient increase gradually, but the change is still small.

4.4 Impact of Crack Depth

In the above-mentioned simulation, to simplify the simulation, the shell-63 unit is selected for the simulation of defects in the same thickness. However, when changing the thickness of defects, the solid-45 unit should be used (Zhou 2006). The crack depth of 1.5mm, 2.0mm, 2.5mm and 3.0mm are simulated, respectively. The relationship between crack widths and transmission coefficients is shown in Fig. 12.

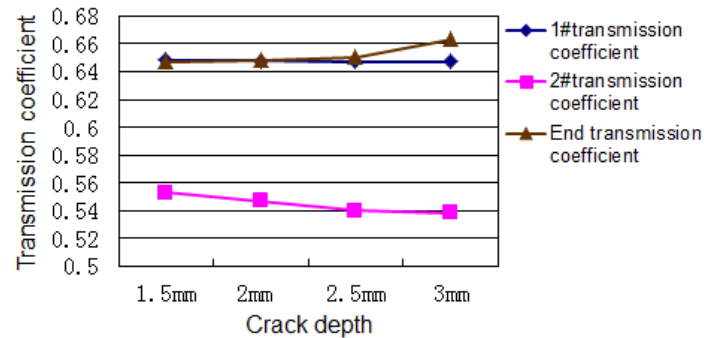


Fig. 12 Transmission coefficients vs. crack depths

From Fig. 12, we can clearly see that, with increase of the crack depth, the defect transmission coefficient decreases gradually, and end transmission coefficient increases gradually.

5. CONCLUSIONS

(1) It is feasible to simulate the pipe crack detection by using PZT-based guided waves. The location of the cracks can be exactly determined through actuating the guided wave with appropriate frequency and modal.

(2) With the increase of the crack degree of central angle, the flaw echo amplitude value increases gradually, the end echo and the defect transmission coefficient decrease gradually, respectively, and end transmission coefficient increases gradually under the condition of the same incident wave amplitude value.

(3) With the increase of the crack width, the amplitude values of two flaw echo increase and the end echo amplitude decrease gradually, but the change is very small. The defect transmission coefficient decrease gradually, end transmission coefficient increase gradually, but the change is still small.

(4) With the increase of the crack depth, the two flaw echo amplitude values increase and the end echo amplitude decrease gradually. The defect transmission coefficients decrease gradually and end transmission coefficients increase gradually.

AKCNOWLEDGEMENT

This work was financially supported in part by the National Natural Science Foundation of China (51278373), and the Natural Science Foundation of Liaoning Province (201202180), the Science Foundation of Liaoning Education Department (L2012214), as well as Liaoning Electric Power Survey & Design Institute Foundation.

REFERENCES

- Du, G.S, Wang, Y.J, Yuan, Y.F. and Zhao, Q.C. (2004), "Axisymmetric guided waves in cylindrical composite structures with weak interfaces," *Acta Physica Sinica*, **18**(1): 27-34. (In Chinese)
- Gazis, D.C. (1959), "Three-dimensional investigation of the propagation of waves in hollow circular cylinders," *Journal of Acoustical Society of America*, **31**(5), 573-578.
- Greenspon, J.E. (1960), "Analysis of wave propagation in a cylindrical waveguide I," *Journal of Acoustical Society of America*, **32**(5), 571-578.
- Greenspon, J.E. (1960), "Analysis of wave propagation in a cylindrical waveguide II," *Journal of Acoustical Society of America*, 1960, **32**(8), 1017-1025.
- Lowe, M.J.S, Alleyne, D. N. and Cawley, P. (1998), "Defect detection in pipes using guided waves," *Ultrasonics*, **36**(1-5), 147-154.
- Lowe, M.J.S., Alleyne, D.N., Cawley, P. (1998), "The mode conversion of a guided wave by a part-circumferential notch in a pipe," *J. Appl. Mech.*, **65**, 649-656.
- Rose, J.L., Cho, Y. and Avioli, M.J. (2009), "Next generation guided wave health monitoring for long range inspection of pipes," *Journal of Loss Prevention in the Process Industries*, **22**(6), 1010-1015.
- Silk, M.G. and Bainton, K.P. (1979), "Propagation in metal tubing of ultrasonic wave modes equivalent to Lamb waves," *Ultrasonics*, **17**(1), 11-19.
- Hong, X.U., Wang, B. and Jiang, X.J. (2009), "Numerical simulation on pipe defect detection using ultrasonic guided waves," *Journal of Power Engineering*, **29**(11), 1019-1022.
- Zang, T.J. and Zang, T.H. (1998), "The general situation of the development of our pipeline transportation," *Pipeline Technology and Equipment*, **4**(6), 48-56.
- Zhou, Y.Q. and Wang, Z.H. (2006), "Numerical simulation of crack detection in pipes using ultrasonic longitudinal guided-wave," *Journal of North University of China (Nature Science Edition)*, **27**(3), 260-269.